



*J. Serb. Chem. Soc.* 84 (10) 1155–1167 (2019)  
JSCS–5254

## Facile solvothermal synthesis of Pt–Cu nanocatalyst with improved electrocatalytic activity toward methanol oxidation

MUHAMMAD HARIS MEHMOOD<sup>1</sup>, MUHAMMAD TARIQ<sup>1\*</sup>, AYAZ HASSAN<sup>2</sup>,  
ABDUL RAZIQ<sup>1</sup>, ABDUR RAHIM<sup>3</sup> and JEHANGEER KHAN<sup>1</sup>

<sup>1</sup>National Centre of Excellence in Physical Chemistry, University of Peshawar-25120, Pakistan, <sup>2</sup>Universidade de São Paulo (USP). Instituto de Química de São Carlos (IQSC), Brazil and <sup>3</sup>Interdisciplinary Research Centre in Biomedical Materials (IRCBM), COMSATS University Islamabad, Lahore Campus, Pakistan

(Received 31 January, revised 7 May, accepted 9 May 2019)

**Abstract:** A binary metal nanocatalyst of platinum and copper was synthesized using a facile solvothermal process (polyol method). The synthesized catalyst was characterized using energy dispersive X-ray spectroscopy (EDS), X-ray diffraction (XRD) and transmission electron microscopy (TEM). The electrochemical performance of the synthesized carbon supported binary metal catalyst, Pt–Cu/C, toward methanol oxidation reaction was checked and then compared with the commercial Pt/C (E-TEK) catalyst, using cyclic voltammetry and chronoamperometric techniques. The Pt–Cu/C catalyst was found to be cubic in shape with indentations on the particle surface, having platinum to copper atomic composition of 4:1, *i.e.*, (Pt<sub>4</sub>Cu). The peak current density for Pt–Cu/C catalyst recorded as 2.3 mA cm<sup>-2</sup> at 0.7 V (*vs* Ag/AgCl) and 50 mV s<sup>-1</sup>, was two times higher than the current density of the commercially available Pt/C catalyst (1.16 mA cm<sup>-2</sup> at 0.76 V). Moreover, the Pt–Cu/C catalyst was found to be more durable than the commercial Pt/C catalyst, as the Pt–Cu/C retained 89 % of its initial current density, while the commercial Pt/C catalyst retained 65 % of its initial current density after 300 potential cycles.

**Keywords:** cyclic voltammetry; electrochemical activity; chronoamperometry; fuel cells; DMFC.

### INTRODUCTION

It is quite evident that energy holds the prime importance for sustaining life. The current source of energy, that meets about 80 % of the world energy demands, is fossil fuels *i.e.*, coal, oil and natural gas.<sup>1</sup> However, fossil fuel reservoirs are limited and the rate at which they are being consumed is alarming. Another crucial problem regarding fossil fuels is that burning of fossil fuels is causing

\* Corresponding author. E-mail: dr.muhammadtariq@uop.edu.pk; tariq\_ftj@yahoo.com  
<https://doi.org/10.2298/JSC190131041M>

adverse environmental problems such as climate change, depletion of ozone layer, air and water pollution, production of toxic wastes, global warming, *etc.*, which in turn, is affecting both humans and wild life. It is due to the fact that on combustion, fossil fuels produce gas compounds like  $\text{SO}_x$  ( $\text{SO}_2$ ,  $\text{SO}_3$ ) and  $\text{NO}_x$  ( $\text{NO}$ ,  $\text{NO}_2$ ), particulate matter which are also known as primary air pollutants and are eventually the reason for the formation of secondary air pollutants *i.e.*, acid rain, smog, *etc.*<sup>2</sup>

Nowadays, based on availability of energy resources, various energy technologies have been developed, for example, there is wind turbine technology to take advantage of wind energy and convert it to electric power which is then used for different purposes. Similarly, water turbines are used to convert hydraulic energy into electricity, solar photovoltaic panels to convert solar energy into electricity, nuclear reactors to generate nuclear energy for several applications. Moreover, batteries, supercapacitors, fuel cells *etc.* are other common types of energy technologies.

Among these various technologies, fuel cells were extensively studied.<sup>3-5</sup> Unlike, batteries, fuel cells directly produce electricity from a fuel, which could either be hydrogen ( $\text{H}_2$ ) or small organic molecules ( $\text{CH}_3\text{OH}$ ,  $\text{C}_2\text{H}_5\text{OH}$ ,  $\text{HCOH}$ , *etc.*). Methanol, as a fuel, has immense potential among other hydrocarbons, due to; its higher electrochemical activity, simpler molecular structure, easy storage and handling as its liquid at room temperature, low production cost than hydrogen as methanol can easily be produced by fermentation of agricultural products and can also be obtained from fossil fuels and from biomasses. Moreover, it also has higher energy density than hydrogen.<sup>6</sup>

A common example of methanol fuel cell is direct methanol fuel cells (DMFCs), in which methanol is directly used in liquid form. The main components of a direct methanol fuel cell include; electrodes (anode and cathode) and a proton conducting membrane. Generally, the anode in DMFCs is composed of platinum or platinum-based materials (Pt–Ru, Pt–Cu, *etc.*).<sup>7</sup>

The basic problem with direct methanol fuel cells (DMFCs) was the adsorption of carbon monoxide and other intermediate species to the catalyst surface. The adsorption of these species slow oxidation process of methanol in direct methanol fuel cells.<sup>8</sup> To overcome this problem, several researcher have adopted the strategy of alloying the platinum with other metals like Ru, Pd,<sup>9</sup> Ir,<sup>10</sup> Pb,<sup>11</sup> Ni,<sup>12</sup> Co,<sup>13</sup> Au,<sup>14</sup> V,<sup>15</sup> Fe<sup>16</sup> and Cu<sup>17-20</sup> whereas, some has fabricated ternary platinum based catalysts for methanol oxidation.<sup>21</sup> It was reported that alloying other metals with platinum makes it more efficient for methanol oxidation reaction (MOR) by changing the electronic structure of platinum by “ligand effect”, which may in turn loosen the strong adsorption affinity of carbon monoxide (CO) on platinum surface and hence less poisoning.<sup>22</sup> The present study, therefore,

demonstrates the facile synthesis, characterizations, and the electrochemical performance of binary Pt–Cu alloy catalyst methanol oxidation.

## EXPERIMENTAL

### *Chemicals and instrumentations*

Chloroplatinic acid hexahydrate ( $\text{H}_2\text{PtCl}_6 \cdot 6\text{H}_2\text{O}$ ,  $\geq 99.9\%$ ) and polyvinylpyrrolidone (PVP, M.wt.~55,000) from Sigma Aldrich, copper chloride dihydrate ( $\text{CuCl}_2 \cdot 2\text{H}_2\text{O}$ , 99%), ethylene glycol (1,2-ethanediol/ $(\text{CH}_2\text{OH})_2$ , extra pure), methanol ( $\text{CH}_3\text{OH}$ ,  $\geq 99.9\%$ ) and sulfuric acid ( $\text{H}_2\text{SO}_4$ , 98%) from Scharlau, Tetra-*n*-butyl ammonium iodide ( $\text{C}_{16}\text{H}_{36}\text{IN}$ , 98%) from Merck Millipore and carbon black (Vulcan XC-72) from Cabot were used in the experimental work. All the reagents were used without further purification. Triply distilled water was used for solution preparation. Both commercial and absolute ethanol was used for washing, along with triply distilled water.

Digi-Ivy potentiostat (DY2100) was used for electrochemical studies, *i.e.*, cyclic voltammetry and chronoamperometry. A conventional three electrode cell system was employed. Silver/silver chloride (saturated KCl) as reference electrode, a glassy carbon electrode (3 mm diameter) fabricated with the prepared catalyst (Pt–Cu) as working electrode and a platinum was used as counter electrode. The preparation of the catalyst was carried out in a reflux condensation assembled round bottom flask, accompanied with oil bath heating *via* magnetic hot plate stirrer.

### *Catalyst preparation*

The catalyst was prepared using polyol method.<sup>23</sup> In a typical synthesis, 7 mL of ethylene glycol was reflux condensed for an hour in a round bottom flask at 180 °C, and that way the solution A was prepared. Meanwhile, 300 mg of tetra-*n*-butyl ammonium iodide ( $\text{C}_{16}\text{H}_{36}\text{IN}$ ) (as shaping agent) was dissolved in 4 mL of ethylene glycol to make solution B. Another solution, consisting a mixture of 250 mg of PVP (polyvinylpyrrolidone) (as protecting agent), 6.8 mg of copper chloride dihydrate ( $\text{CuCl}_2 \cdot 2\text{H}_2\text{O}$ ) and 0.5 mL of chloroplatinic acid hexahydrate ( $\text{H}_2\text{PtCl}_6 \cdot 6\text{H}_2\text{O}$ , 77.23 mM in  $\text{H}_2\text{O}$ ) in another 4 mL of ethylene glycol was prepared and was named solution C. The amounts of platinum (Pt) and copper (Cu) salts were taken in a way so that it could be in 1:1 mole ratio in the reaction mixture. After one hour of reflux condensation of solution A was complete, solution B was also added to the round bottom flask with continuous stirring. After that, solution C was added dropwise to the round bottom flask, which was completed in 5 min. The reaction was then allowed to take place for 90 min after the addition of last solution (solution C). The reaction vessel was then removed from the oil bath and was allowed to cool down at room temperature. The product was then separated by centrifugation, washed several times using triply distilled water/ethanol and was finally dispersed in ethanol.

The prepared catalyst was then supported on a carbon clack (Vulcan XC-72). Both the particles and carbon support were dispersed by sonication for 30 min in ethanol, then both were mixed and again dispersed for another 30 min. The mixture was then subjected to stirring for 72 h.<sup>9,24</sup> The supported particles were then filtered and dried overnight in an oven at 80 °C. The product was then stored in air tight vials for further physical and electrochemical characterization.

### *Electrochemical measurements*

The working electrode was fabricated with the prepared catalyst using the following method. First, the catalyst dispersion was prepared by sonicating the nanoparticles (0.6 mg

$\text{mL}^{-1}$ ) in ethanol for 20 to 30 min. The catalyst dispersion (10  $\mu\text{L}$ ) was then drop casted on glassy carbon electrode (GCE) and was allowed to dry at room temperature. Once dried, 10  $\mu\text{L}$  of 0.05 % Nafion (proton exchange membrane) was drop casted above the dried catalyst layer on glassy carbon electrode and was again allowed to dry at room temperature. Prior to the fabrication of GCE, it was thoroughly washed and cleaned till the clear glossy appearance of its surface. The GCE was polished with alumina powder slurry, then sonicated and was finally rinsed with distilled water and acetone/ethanol. All the electrochemical measurements were performed at room temperature in acidic medium (0.5 M  $\text{H}_2\text{SO}_4$ ) and at a scan rate of 50  $\text{mV s}^{-1}$ . The experimental setup for electrochemical measurement is shown in Fig. S-2 of the Supplementary material to this paper.

## RESULT AND DISCUSSION

### *Characterization of Pt–Cu/C nanoparticles*

**EDS analysis.** Elemental analysis of the as prepared catalyst was done by energy-dispersive X-ray spectroscopy. Fig. 1 shows the EDS spectrum for the as prepared particles. EDS data reveals that the percent weight of carbon, platinum and copper is 76.7, 18.63 and 4.37 %, respectively. According to the observed percent weight composition it can be inferred that the percent weight ratio between carbon and as prepared catalyst was  $\sim 77(\text{C}):23(\text{Pt–Cu})$ . A small oxygen peak can also be seen in the EDS spectrum which may be attributed to some impurities or may be to surface oxide formation because of the aging of nanoparticles in open atmosphere.

The weight percentage between Pt and Cu in the as prepared catalyst was 93.2 and 6.8 %, respectively. This weight ratio suggests that in terms of atomic ratio, the percentage of Pt and Cu is  $\sim 81$  and 19 %, respectively (*i.e.*,  $\sim 4:1$ ,  $\text{Pt}_4\text{Cu}$ ). As mentioned in the catalyst preparation method, the parent mole ratio of precursor salts ( $\text{H}_2\text{PtCl}_6 \cdot 6\text{H}_2\text{O}:\text{CuCl}_2 \cdot 2\text{H}_2\text{O}$ ) taken for the nanoparticle synthesis was 1:1, however, the experimental composition of the product turned out to be  $\sim 4:1$ . It can be determined that using the method employed in this work, if an equimolar parent mole ratio of the respective precursor salts is taken, an approximate 4:1 (Pt:Cu) can be achieved in the product.

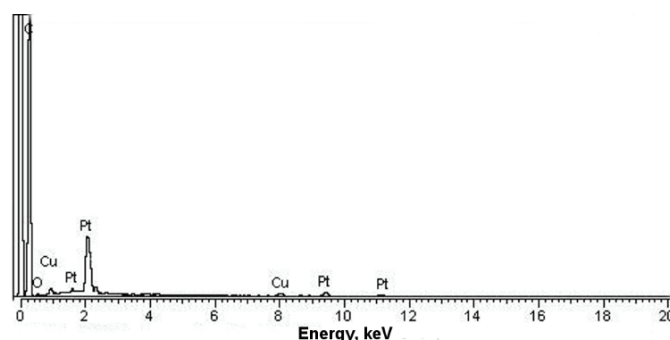


Fig. 1. EDS spectrum of the as prepared Pt–Cu/C catalyst.

**XRD analysis.** X-Ray diffractogram for the Pt–Cu/C catalyst is given in Fig. 2. It was observed from the XRD pattern that the catalyst is highly crystalline. The XRD peak positions for pure platinum (JCPDS No. 04-0802) and copper particles (JCPDS No. 153 85-1326) for the facets (111), (200) and (220) are mentioned by vertical line marking in Fig. 2a. The shifting of the peaks from the pure metallic components (*i.e.*, platinum and copper) of the catalyst is attributed to the formation of alloy catalyst, *i.e.*, incorporating other atoms of smaller or larger atomic radii in the lattice of a crystal shifts the diffraction peaks towards larger or smaller theta ( $2\theta$ ) angles, respectively. As the atomic radius of copper is smaller (145 pm) than platinum (175 pm), it can be seen in Figs. 2a and b that the Pt peak has shifted towards higher angle theta, supporting the claim that Cu has been alloyed with platinum in the particles. The XRD results are also in accordance with the EDS results, *i.e.*, the elemental analysis shows that incorporation of both parent metals in terms of platinum to copper is approximately 4:1 ( $\sim$ Pt<sub>4</sub>Cu) and the peak shifting is in accordance with these results.

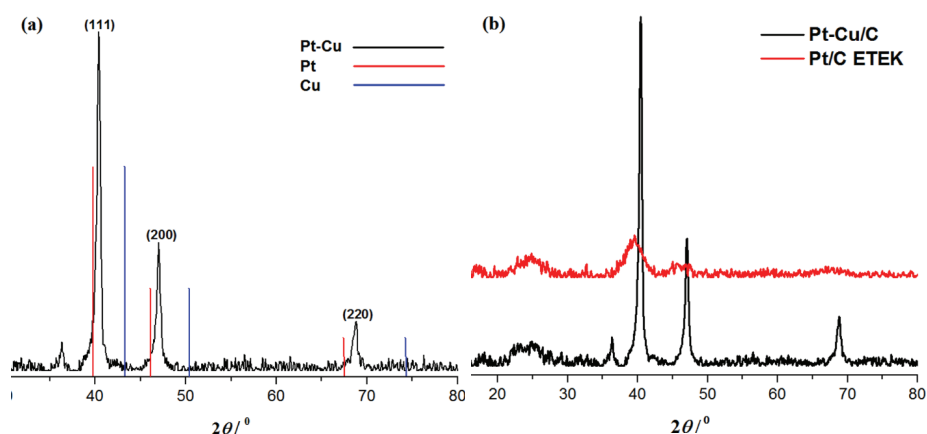


Fig. 2. a) XRD Peak positions for Pt–Cu, Pt and Cu; b) XRD spectra of Pt–Cu/C in comparison with Pt/C.

A small diffraction peak can also be seen just before the Pt–Cu (111) peak. It refers to the formation of some Cu<sub>2</sub>O (JCPDS No.73-2076), either due to the ambient synthesis conditions, or due to the aging of nanoparticles in open atmosphere, as mentioned earlier in EDS section.

**TEM analysis.** TEM images of the Pt–Cu/C catalyst are shown in Fig. 3. The approximate shape and size of the synthesized Pt–Cu nanoparticles were determined from these images. Although the mechanism was not determined, the iodides and the cation part (C<sub>16</sub>H<sub>36</sub>N<sup>+</sup>) of the salt used are supposed to be responsible for the shape of the particle. The major shape of the particles was cubic with

the indentation on the surface running deep within the particles. The observed particle size, as observed from the TEM images, is around 25–30 nm.

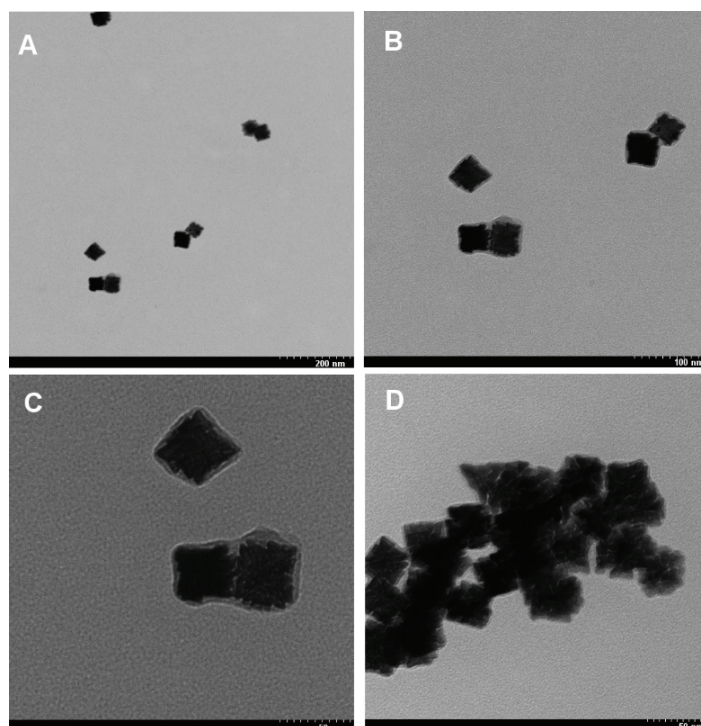


Fig. 3. TEM image of the Pt–Cu/C catalyst at various magnification.

The surface area of the catalyst available for the electrochemical electron transfer reaction is called electrochemically active surface area or electrochemical surface area (*ECSA*). Determination of *ECSA* is a principal factor which must be known, in order to evaluate the current density and for comparison of the newly developed electrocatalyst with the standard or commercially available catalyst. *ECSA* is expressed as the surface area of the electrocatalyst per unit mass or per unit loading of the electrocatalyst, *i.e.*,  $\text{m}^2 \text{g}^{-1}$  or  $\text{cm}^2 \text{mg}^{-1}$ .

There are two well-known methods for the determination of the electrochemically active surface area of Pt electrocatalysts, *i.e.*, hydrogen adsorption-desorption method and carbon monoxide oxidation method.<sup>25,26</sup> The hydrogen adsorption-desorption method (also called hydrogen under-potential deposition method) is used more frequently for *ECSA* determination of electrocatalyst as compared to the carbon monoxide adsorption method (CO-stripping method).<sup>27</sup> This is due to the reason that in case of hydrogen adsorption, monolayer formation is supposed to be more reliable than in case of carbon monoxide adsorption, because there is also possibility of bridging the adsorption of carbon monoxide



on catalyst surface, occupying two adsorption sites of the catalyst surface leading to less precise results.<sup>25</sup>

In the present work, the hydrogen adsorption-desorption method was used for the determination of surface area of the as prepared catalyst. There are normally three regions that can be observed in a cyclic voltammogram of a platinum electrode in acidic solution, *i.e.*, hydrogen region, double layer region and oxygen region, as shown (supporting Fig. S-4 of the Supplementary material).<sup>27</sup> In this method the area under the curve of hydrogen adsorption peak (hydrogen region), obtained by cyclic voltammetry, is integrated and the total amount of charge obtained by the monolayer adsorption (electrochemical chemisorption) is calculated, which is then used to determine the electrochemically active surface area (Fig. 4).<sup>28</sup>

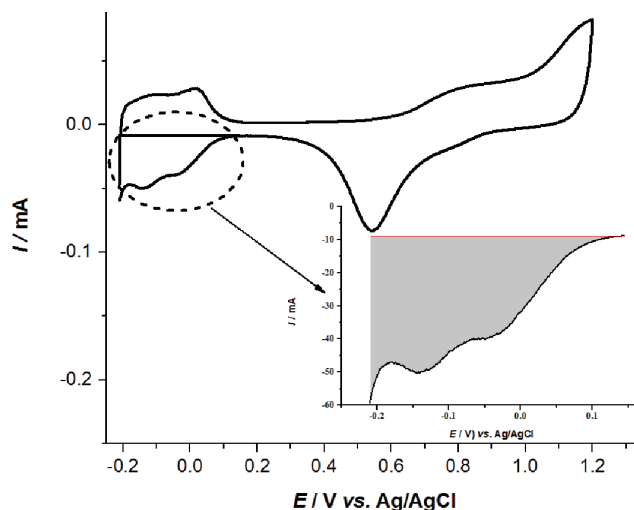


Fig. 4. CV scan for the ECSA determination of Pt-Cu/C nanoparticles. Inset shows integrated area for hydrogen adsorption charge.

The following equation was used to determine the electrochemically active surface area:<sup>29</sup>

$$ECSA = \frac{Q_m}{m_{Pt} Q_d} \quad (1)$$

where  $Q_m$  is the charge obtained for the hydrogen monolayer adsorption,  $m_{Pt}$  is the platinum catalyst loading and  $Q_d$  is the value of charge density for platinum surface to reduce monolayer of hydrogen, which is based on the assumption that one hydrogen atom is adsorbed (chemisorbed) on one platinum atom.  $Q_d$  has a value of  $\sim 210 \mu\text{C cm}^{-2}$ .<sup>30</sup>

A stable cyclic voltammogram was considered *ECSA* determination of the as prepared Pt–Cu nanoparticles. The area under the hydrogen adsorption curve was integrated using OriginPro9 to obtain the charge consumed for the monolayer adsorption of hydrogen on the Pt–Cu/C electrocatalyst. The *ECSA* obtained according to Eq. (1) was  $12.5 \text{ m}^2 \text{ g}^{-1}$ .

The *ECSA* of Pt–Cu/C catalyst determined by the hydrogen adsorption desorption method refers to platinum and not for copper.

#### *Methanol electrooxidation on Pt–Cu catalyst*

The electrochemical activity of the prepared Pt–Cu/C catalyst was evaluated towards methanol oxidation reaction (MOR) through cyclic voltammetry (Fig. 5). CV experiments were performed in 0.5 M  $\text{H}_2\text{SO}_4$  containing 1 M methanol at  $50 \text{ mV s}^{-1}$  in a potential range of  $-0.2$  to  $1.2 \text{ V}_{\text{Ag}/\text{AgCl}}$ . The commercially available Pt/C (EOTEK) catalyst was used as reference. It can be observed in that the onset potential for the methanol electrooxidation has been very slightly shifted towards more negative potential, than the onset potential of the reference Pt/C catalyst, depicting that the as prepared catalyst is kinetically active towards methanol electrooxidation. The current peak potential for MOR of the Pt–Cu/C catalyst was  $0.7 \text{ V}$  as compared to the higher current peak potential value of reference Pt/C catalyst which was  $0.76 \text{ V}_{\text{Ag}/\text{AgCl}}$ . Moreover, it can also be observed that the Pt–Cu/C catalyst had shown better electrocatalytic activity towards MOR in terms of current density ( $j$ ), *i.e.*,  $2.3 \text{ mA cm}^{-2}$  for Pt–Cu/C and  $1.15 \text{ mA cm}^{-2}$  for Pt/C reference catalyst. Although there is only a slight shift in the onset potential, the overall performance in terms of the current density and the current peak potential implicates better electrocatalytic activity of the prepared Pt–Cu/C catalyst than the commercial Pt/C catalyst. As mentioned earlier that the enhanced

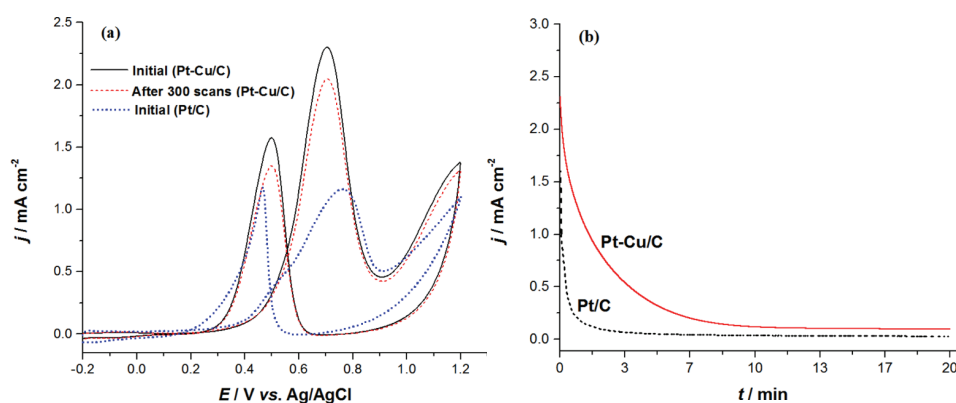


Fig. 5. a) Cyclic voltammograms showing reduction in catalytic activity of the prepared Pt–Cu/C catalyst after 300 scans in comparison with the initial electrocatalytic activity of Pt/C catalyst; b) chronoamperometric curves for Pt–Cu/C and Pt/C catalyst for durability test.



activity of Pt-Cu/C catalyst is, definitely, due to the alloying of platinum with copper which may be attributed to the “ligand effect”, by which copper donates its electrons to platinum which occupy the d-orbitals of platinum, reducing the interactive forces between platinum and carbon monoxide (and other intermediate species), hence, less poisoning and improved electrocatalytic activity towards MOR.<sup>22,31</sup> The alloying of nanoparticles also produces strain in the catalyst (called “strain effect”), distorting the electronic structure of the catalyst nanoparticles, which in turns further improves the electrocatalytic activity. This factor may also be responsible for the better electrocatalyst activity of Pt-Cu nanoparticles towards methanol electrooxidation.<sup>22</sup>

The peak current obtained in the forward scan ( $I_F$ ) of CV is due to the electrooxidation of methanol and the peak current obtained in the reverse scan ( $I_B$ ) of CV is also due to the oxidation of methanol on the surface freed from the accumulated intermediate species (*i.e.*,  $\text{HCO}^-$ ,  $\text{CO}$ ,  $\text{HCOO}^-$ ) formed during methanol oxidation in the forward scan.<sup>32</sup> The intermediate species, specially carbon monoxide (CO), act as poison for the catalyst.<sup>33</sup> The ratio of the forward peak current and the backward peak current is often used to determine the tolerance of a catalyst against the intermediate species formed in the forward scan during methanol oxidation.<sup>34</sup> It can be observed from Figure 4 that the ratio  $I_F/I_B$  obtained for the Pt-Cu/C catalyst was also found to be higher,  $(I_F/I_B)_{\text{Pt-Cu}} = 1.5$ , than the ratio obtained for the commercial Pt/C catalyst,  $(I_F/I_B)_{\text{Pt/C}} = 0.98$ , presenting the better tolerance of the Pt-Cu/C catalyst against intermediate poisoning species. The summarized values for different parameters are given in Table I.

TABLE I. Summarized values of different parameters for the as prepared Pt-Cu catalyst in comparison with commercial Pt/C catalyst and already reported Pt-Cu (HBND) and Pt-Ru/C catalyst<sup>17</sup>

Parameter	Pt-Cu/C <sup>a</sup>	Pt/C(Commercial) <sup>a</sup>	Pt-Cu <sup>b</sup>	Pt-Ru/C <sup>b</sup>
Onset potential ( $E_{\text{onset}}$ ), $\text{V}_{\text{Ag}/\text{AgCl}}$	0.45	0.47	0.44	0.43
Peak potential ( $E_p$ ), $\text{V}_{\text{Ag}/\text{AgCl}}$	0.7	0.76	0.68	0.64
Current density (initial), $\text{mA cm}^{-2}$	2.3	1.16	1.38	0.70
Current density after 300 scans, $\text{mA cm}^{-2}$	2.04	0.75	1.25	–
Ratio ( $I_F/I_B$ )	1.5	0.98	1.17	1.92

<sup>a</sup>Value obtained from this work, <sup>b</sup>approximate value obtained from ref. 17

A catalyst for electrochemical oxidation of methanol, especially for fuel cells, must be durable enough for its practical application.<sup>35</sup> Chronoamperometry was employed to evaluate the durability of the prepared Pt-Cu/C catalyst in comparison with the commercial Pt/C catalyst. In chronoamperometry the catalyst is tested at a certain fixed potential for extended time spans. The measurements were performed in 0.5 M  $\text{H}_2\text{SO}_4$  containing 1 M methanol at a potential of 0.65  $\text{V}_{\text{Ag}/\text{AgCl}}$  for 20 min. The current decline observed in Fig. 5b is due to the

accumulation of intermediate species, acting as catalyst poison, formed as a result of methanol oxidation.<sup>36</sup> Fig. 5b also depicts the comparison of chronoamperometric curves of the prepared catalyst with Pt/C catalyst. Although a rapid decline in current densities for both the catalysts can be observed, but the rate of decline in the case of the prepared catalyst is less rapid than the Pt/C reference catalyst, being more kinetically favourable towards methanol oxidation and owing to the better tolerance of the prepared catalyst against intermediate poisoning species. Furthermore, it can be observed that the current density of the as prepared catalyst remained higher than the Pt/C catalyst during the given time span.

The stability of the prepared catalyst was also investigated using cyclic voltammetry in 0.5 M H<sub>2</sub>SO<sub>4</sub>, 1 M methanol at 50 mV s<sup>-1</sup> for 300 scans. It was observed that after 300 cycles the peak current of the as prepared catalyst reduced by 11.3 %, which has still a higher peak current value than the initial peak current value of commercial Pt/C catalyst, as can be seen in Fig. 5a.

The current densities and the losses in them after potential cycling for both the prepared Pt–Cu/C catalyst and commercial Pt/C catalyst were plotted as bar graphs and are presented in Fig. 6. It was observed that current density for the prepared catalyst got reduced by 11.3 %, while for Pt/C catalyst it was reduced by 35.3 % after 300 CV cycles.

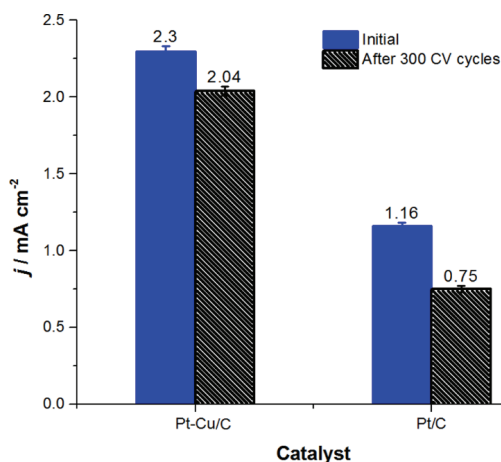


Fig. 6. Bar graph showing loss in current densities of Pt–Cu/C catalyst vs. Pt/C catalyst.

#### CONCLUSION

Pt–Cu/C catalyst was synthesized successfully via facile solvothermal process having improved electrocatalytic activity toward methanol oxidation. The electrocatalyst was characterized using EDX, XRD, TEM, cyclic voltammetry, and chronoamperometry techniques. The quantities, such as onset potential ( $E_{\text{onset}}$ ), peak potential ( $E_f$ ), current density ( $j$ ), durability and tolerance to intermediate species ( $I_F/I_B$ ), for the synthesized Pt–Cu/C catalyst are comparable with

Pt–Ru/C electrocatalyst (a standard electrocatalyst for MOR) and even better than the commercially available Pt/C catalyst.

*Acknowledgements.* Higher Education Commission of Pakistan is acknowledged for funding, while CABOT Corporation and Mr. Shakil Ahmed are highly acknowledged for providing us Vulcan XC72 free of cost for this work.

## ИЗВОД

ЈЕДНОСТАВНА СИНТЕЗА НАНОКАТАЛИЗАТОРА Pt–Cu СА ПОБОЉШАНОМ АКТИВНОШЋУ ЗА ОКСИДАЦИЈУ МЕТАНОЛА

MUHAMMAD HARIS, MEHMOOD<sup>1</sup>, MUHAMMAD TARIQ<sup>1</sup>, AYAZ HASSAN<sup>2</sup>, ABDUL RAZIQ<sup>1</sup>, ABDUR RAHIM<sup>3</sup> и JEHANGEER KHAN<sup>1</sup>

<sup>1</sup>National Centre of Excellence in Physical Chemistry, University of Peshawar- 25120. Pakistan, <sup>2</sup>Universidade de São Paulo (USP). Instituto de Química de São Carlos (IQSC), Brazil и <sup>3</sup>Interdisciplinary Research Centre in Biomedical Materials (IRCBM), COMSATS University Islamabad, Lahore Campus, Pakistan

Бинарни метални нанокатализатор платине и бакра синтетисан је једноставним солвотермалним поступком (полиолна метода). Синтетисани катализатор је окарактерисан енергетском дисперзионом спектроскопијом X-зрака (EDS), дифракцијом X-зрака (XRD) и трансмисионом електронском микроскопијом (ТЕМ). Испитана је електрохемијска активност синтетисаног катализатора Pt–Cu/C за реакцију оксидације метанола и упоређена са комерцијалним катализатором Pt/C (ЕТЕК). Коришћене су методе цикличне волтаметрије и хроноамперометрије. Утврђено је да су честице Pt–Cu кубног облика са удубљењима на површини и да је њихов атомски састав Pt:Cu = 4:1, односно Pt<sub>4</sub>Cu. Струјни максимум на волтамограму оксидације метанола снимљеном при брзини 50 mV s<sup>-1</sup> јавља се на потенцијалу 0,7 V (према Ag/AgCl електроди) и има вредност 2,3 mA cm<sup>-2</sup>, што је два пута већа густина струје него на комерцијалном катализатору Pt/C (1,16 mA cm<sup>-2</sup> на 0,76 V<sub>Ag/AgCl</sub>). Поред тога, катализатор Pt–Cu/C је показао већу трајност од комерцијалног Pt/C, јер је у условима циклизирања потенцијала након 300 циклуса задржао 89 % од своје почетне активности, а Pt/C свега 65 %.

(Примљено 31 јануара, ревидирано 7 маја, прихваћено 9. маја 2019)

## REFERENCES

1. C. A. S. Hall, J. G. Lambert, S. B. Balogh, *Energy Policy* **64** (2014) 141 (<http://dx.doi.org/10.1016/j.enpol.2013.05.049>)
2. K. Wang, R. Sripathoorat, S. Luo, M. Tang, H. Du, P. K. Shen, *J. Mater. Chem., A* **4** (2016) 13425 (<http://dx.doi.org/10.1039/c6ta05230d>).
3. J. Larminie, A. Dicks, *Proton Exchange Membrane Fuel Cells: Review*, in *Prot. Exch. Membr. Fuel Cells*, Springer International Publishing AG, 2018, pp. 9 (<http://dx.doi.org/10.1002/9781118878330.ch4>)
4. D. L. Douglas, *Molten Carbonate Cells with Gas-Diffusion Electrodes*, in S. Basu (Ed.), *Recent Trends Fuel Cell Sci. Technol.*, Springer, 1960, pp. 308 (<http://dx.doi.org/10.1021/ie50604a030>)
5. B. C. H. Steele, A. Heinzl, *Nature* **414** (2001) 345 (<http://dx.doi.org/10.1038/35104620>)
6. W. Qian, D. P. Wilkinson, J. Shen, H. Wang, J. Zhang, *J. Power Sources* **154** (2006) 202 (<http://dx.doi.org/10.1016/j.jpowsour.2005.12.019>)
7. X. Zhang, K-Yu. Chan, *Chem. Mater.* **15** (2003) 454 (<https://pubs.acs.org/doi/pdf/10.1021/cm0203868>)

8. B. Beden, C. Lamy, A. Bewick, K. Kunimatsu, *J. Electroanal. Chem.* **121** (1981) 343 ([http://dx.doi.org/10.1016/S0022-0728\(81\)80590-6](http://dx.doi.org/10.1016/S0022-0728(81)80590-6))
9. F. Zhan, T. Bian, W. Zhao, H. Zhang, M. Jin, D. Yang, *CrystEngComm* **16** (2014) 2411 (<http://dx.doi.org/10.1039/C3CE42362J>)
10. P. Holt-hindle, Q. Yi, G. Wu, K. Koczur, A. Chen, *J. Electrochem. Soc.* **155** (2008) K5 (<http://dx.doi.org/10.1149/1.2801987>)
11. J. Wang, P. Holt-Hindle, D. MacDonald, D. F. Thomas, A. Chen, *Electrochim. Acta* **53** (2008) 6944 (<http://dx.doi.org/10.1016/j.electacta.2008.02.028>)
12. Q. Jiang, L. Jiang, H. Hou, J. Qi, S. Wang, G. Sun, *J. Phys. Chem., C* **114** (2010) 19714 (<http://dx.doi.org/10.1021/jp1039755>)
13. D. Wang, H. L. Xin, R. Hovden, H. Wang, Y. Yu, D. A. Muller, F. J. Disalvo, H. D. Abruña, *Nat. Mater.* **12** (2013) 81 (<http://dx.doi.org/10.1038/nmat3458>)
14. W. Tang, S. Jayaraman, T. F. Jaramillo, G. D. Stucky, E. W. McFarland, *J. Phys. Chem., C* **113** (2009) 5014 (<http://dx.doi.org/10.1021/jp8089209>)
15. P. Justin, G. R. Rao, *Catal. Today* **141** (2009) 138 (<http://dx.doi.org/10.1016/j.cattod.2008.03.019>)
16. J. H. Jang, E. Lee, J. Park, G. Kim, S. Hong, Y. U. Kwon, *Sci. Rep.* **3** (2013) 2872 (<http://dx.doi.org/10.1038/srep02872>)
17. Y. Cao, Y. Yang, Y. Shan, Z. Huang, *ACS Appl. Mater. Interfaces* **8** (2016) 5998 (<http://dx.doi.org/10.1021/acsami.5b11364>)
18. G. Fu, X. Yan, Z. Cui, D. Sun, L. Xu, Y. Tang, J. B. Goodenough, J.-M. Lee, *Chem. Sci.* **7** (2016) 5414 (<http://dx.doi.org/10.1039/C6SC01501H>)
19. I. A. Khan, Y. Qian, A. Badshah, D. Zhao, M. A. Nadeem, *Fabrication of Highly Stable and Efficient PtCu Alloy Nanoparticles on Highly Porous Carbon for Direct Methanol Fuel Cells*, 2016 (<http://dx.doi.org/10.1021/acsami.6b06068>)
20. S. Chen, H. Su, Y. Wang, W. Wu, J. Zeng, *Angew. Chem. Int. Ed.* **54** (2015) 108 (<http://dx.doi.org/10.1002/anie.201408399>)
21. A. Chen, P. Holt-Hindle, *Chem. Rev.* **110** (2010) 3767 (<http://dx.doi.org/10.1021/cr9003902>)
22. M. Luo, S. Guo, *Nat. Rev. Mater.* **2** (2017) 1 (<http://dx.doi.org/10.1038/natrevmats.2017.59>)
23. M. Perullini, S. A. Aldabe Bilmes, M. Jobbágy, *Cerium oxide nanoparticles: Structure, applications, reactivity, and eco-toxicology*, Springer, London, 2013 (<http://dx.doi.org/10.1007/978-1-4471-4213-3>)
24. K. Wang, R. Sriphathoorat, S. Luo, M. Tang, H. Du, P. K. Shen, Y. Wang, C. Ma, Z. Li, J. Zeng, *J. Mater. Chem., A* **4** (2016) 13425 (<http://dx.doi.org/10.1039/C6TA05230D>)
25. M. Lukaszewski, M. Soszko, A. Czerwiński, *Int. J. Electrochem. Sci.* **11** (2016) 4442 (<http://dx.doi.org/10.20964/2016.06.71>)
26. T. Binninger, E. Fabbri, R. Kotz, T. J. Schmidt, *J. Electrochem. Soc.* **161** (2013) H121 (<http://dx.doi.org/10.1149/2.055403jes>)
27. J. M. D. Rodríguez, J. A. H. Melián, and J. P. Peña, *J. Chem. Educ.* **77** (2000) 1195 (<https://pubs.acs.org/doi/pdf/10.1021/ed077p1195>)
28. Z. Dongping, J. Velmurugan, M. V. Mirkin, *J. Am. Chem. Soc.* **131** (2009) 14756 (<http://dx.doi.org/10.1021/ja902876v>)
29. A. B. Bocarsly, *Cyclic Voltammetry*, in E. N. Kaufmann (Ed.), *Charact. Mater.*, 2002, pp. 837 (<http://dx.doi.org/10.1002/0471266965.com050.pub2>)
30. S. Gu, W. Sheng, R. Cai, S. M. Alia, S. Song, K. O. Jensen, Y. Yan, *Chem. Commun.* **49** (2013) 131 (<http://dx.doi.org/10.1039/C2CC34862D>)

31. L. Han, P. Cui, H. He, H. Liu, Z. Peng, J. Yang, *J. Power Sources* **286** (2015) 488 (<http://dx.doi.org/10.1016/j.jpowsour.2015.04.003>).
32. S. Du, Y. Lu, R. Steinberger-Wilckens, *Carbon N. Y.* **79** (2014) 346 (<http://dx.doi.org/10.1016/j.carbon.2014.07.076>).
33. D. Y. Chung, H. Il Kim, Y. H. Chung, M. J. Lee, S. J. Yoo, A. D. Bokare, W. Choi, Y. E. Sung, *Sci. Rep.* **4** (2014) 194 (<http://dx.doi.org/10.1038/srep07450>).
34. M. Xiao, S. Li, X. Zhao, J. Zhu, M. Yin, C. Liu, W. Xing, *ChemCatChem* **6** (2014) 2825 (<http://dx.doi.org/10.1002/cctc.201402186>).
35. A. Ghosh, S. Ramaprabhu, *Catal. Sci. Technol.* **7** (2017) 5079 (<http://dx.doi.org/10.1039/C7CY01522D>).
36. H. H. Li, S. Zhao, M. Gong, C. H. Cui, D. He, H. W. Liang, L. Wu, S. H. Yu, *Angew. Chem. Int. Ed.* **52** (2013) 7472 (<http://dx.doi.org/10.1002/anie.201302090>).